

Electronic theory for the normal state spin dynamics in Sr_2RuO_4 : anisotropy due to spin-orbit coupling

I. Eremin^{1,2}, D. Manske¹, and K. H. Bennemann¹

¹ Institut für Theoretische Physik, Freie Universität Berlin, D-14195 Berlin, Germany

² Physics Department, Kazan State University, 420008 Kazan, Russia
(December 27, 2021)

Using a three-band Hubbard Hamiltonian we calculate within the random-phase approximation the spin susceptibility, $\chi(q)$, and NMR spin-lattice relaxation rate, $1/T_1$, in the normal state of the triplet superconductor Sr_2RuO_4 and obtain quantitative agreement with experimental data. Most importantly, we find that due to spin-orbit coupling the out-of-plane component of the spin susceptibility χ^z becomes at low temperatures two times larger than the in-plane one. As a consequence strong incommensurate antiferromagnetic fluctuations of the quasi-one-dimensional xz - and yz -bands point into the z -direction. Our results provide further evidence for the importance of spin fluctuations for triplet superconductivity in Sr_2RuO_4 .

74.20Mn, 74.25.-q, 74.25Ha

The spin-triplet superconductivity with $T_c = 1.5\text{K}$ observed in layered Sr_2RuO_4 seems to be a new example of unconventional superconductivity [1]. The non-s-wave symmetry of the order parameter is observed in several experiments (see for example [2,3]). Although the structure of Sr_2RuO_4 is the same as for the high- T_c superconductor $\text{La}_{2-x}\text{Sr}_x\text{CuO}_4$, its superconducting properties resemble those of superfluid ^3He . Most recently it was found that the superconducting order parameter is of p-wave type, but contains line nodes half-way between the RuO_2 -planes [4,5]. These results support Cooper-pairing via spin fluctuations as one of the most probable mechanism to explain the triplet superconductivity in Sr_2RuO_4 . Therefore, theoretical and experimental investigations of the spin dynamics behavior in the normal and superconducting state of Sr_2RuO_4 are needed.

Recent studies by means of inelastic neutron scattering (INS) [6] and nuclear magnetic resonance (NMR) [7] of the spin dynamics in Sr_2RuO_4 reveal the presence of strong incommensurate fluctuations in the RuO_2 -plane at the antiferromagnetic wave vector $Q_1 = (2/3; 2/3)$. As it was found in band structure calculations [8], they result from the nesting properties of the quasi-one-dimensional d_{xz} - and d_{yz} -bands. The two-dimensional d_{xy} -band contains only weak ferromagnetic fluctuations. The observation of the line nodes between the RuO_2 -planes [4,5] suggests strong spin fluctuations between the RuO_2 -planes in z -direction [9,11]. However, inelastic neutron scattering [12] observes that magnetic fluctuations are purely two-dimensional and originate from the RuO_2 -plane. Both behaviors could result as a consequence of the magnetic anisotropy within the RuO_2 -plane as indeed was observed in recent NMR experiments by Ishida et al. [13]. In particular, analyzing the temperature dependence of the nuclear spin-lattice relaxation rate on ^{17}O in the RuO_2 -plane at low temperatures, they have demonstrated that the out-of-plane component of the spin susceptibility can become almost three times larger than the

in-plane one. This strong and unexpected anisotropy disappears with increasing temperature [13].

In this Communication we analyze the normal state spin dynamics of the Sr_2RuO_4 using the two-dimensional three-band Hubbard Hamiltonian for the three bands crossing the Fermi level. We calculate the dynamical spin susceptibility $\chi(q)$ within the random-phase approximation and show that the observed magnetic anisotropy in the RuO_2 -plane arises mainly due to the spin-orbit coupling. Its further enhancement with lowering temperatures is due to the vicinity to a magnetic instability. Thus, we demonstrate that as in the superconducting state [14] the spin-orbit coupling plays an important role also for the normal state spin dynamics of Sr_2RuO_4 . We also discuss briefly the consequences of this magnetic anisotropy for Cooper-pairing due to the exchange of spin fluctuations.

We start from the two-dimensional three-band Hubbard Hamiltonian

$$H = H_t + H_U = \sum_{k,l} \sum_{i,j} t_{k,l} a_{k,l}^\dagger a_{i,j} + \sum_{i,l} U_1 n_{i,l} n_{i,l}^\dagger; \quad (1)$$

where $a_{k,l}$ is the Fourier-transformed annihilation operator for the d_l orbital electrons ($l = xy, yz, zx$) and U_1 is the corresponding on-site Coulomb repulsion. $t_{k,l}$ denotes the energy dispersions of the tight-binding bands calculated as follows: $t_{k,l} = \epsilon_0 - 2t_x \cos k_x - 2t_y \cos k_y + 4t^0 \cos k_x \cos k_y$. We choose the values for the parameter set $(\epsilon_0; t_x; t_y; t^0)$ as $(0.5, 0.42, 0.44, 0.14)$, $(0.24, 0.31, 0.045, 0.01)$, and $(0.24, 0.045, 0.35, 0.01)\text{eV}$ for d_{xy} , d_{yz} , and d_{zx} -orbitals in accordance with band-structure calculations [15]. The electronic properties of this model in application to Sr_2RuO_4 were studied recently and as was found can explain some features of the spin excitation spectrum in Sr_2RuO_4 [8,14,16,11]. However, this model fails to explain the observed magnetic anisotropy at low temperatures [13] and line nodes in the superconducting

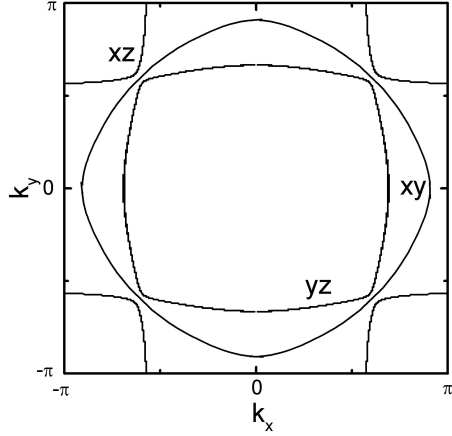


FIG. 1. Calculated Fermi surface for a RuO_2 plane in Sr_2RuO_4 taking into account spin-orbit coupling.

order parameter below T_c which are between the RuO_2 -planes. On the other hand, it is known that the spin-orbit coupling plays an important role in the superconducting state of in Sr_2RuO_4 [14]. This is further confirmed by the recent observation of the large spin-orbit coupling in the insulating Ca_2RuO_4 [17]. Therefore, we include in our model spin-orbit coupling:

$$H_{\text{so}} = \sum_i \mathbf{L}_i \mathbf{S}_i ; \quad (2)$$

where the angular momentum \mathbf{L}_i operates on the three t_{2g} -orbitals on the site i . Similar to an earlier approach [14], we restrict ourselves to the three orbitals, ignoring e_{2g} -orbitals and choose the coupling constant such that the t_{2g} -states behave like an $l = 1$ angular momentum representation. Moreover, it is known that the quasi-two-dimensional xy -band is separated from the quasi-one-dimensional xz - and yz -bands. Then, one expects that the effect of spin-orbit coupling is small and can be excluded for simplicity. Therefore, we consider the effect of the spin-orbit coupling on xz - and yz -bands only. Then, the kinetic part of the Hamiltonian $H_t + H_{\text{so}}$ can be diagonalized and the new energy dispersions are

$$\begin{aligned} \epsilon_{k,yz} &= (t_{k,yz} + t_{k,xz} + A_k) = 2 \\ \epsilon_{k,xz} &= (t_{k,yz} + t_{k,xz} - A_k) = 2 \end{aligned} \quad (3)$$

where $A_k = \frac{P}{(t_{k,yz} - t_{k,xz})^2 + 2}$, and P refers to spin projection. One clearly sees that the spin-orbit coupling does not remove the Kramers degeneracy of the spins. Therefore, the resultant Fermi surface consists of three sheets like observed in the experiment. Most importantly, spin-orbit coupling together with Eq. (1) leads to a new quasiparticle which we label by pseudo-spin and pseudo-orbital indices. The unitary transformation U_k connecting old and new quasiparticles is defined for each wave vector and lead to the following relation between them :

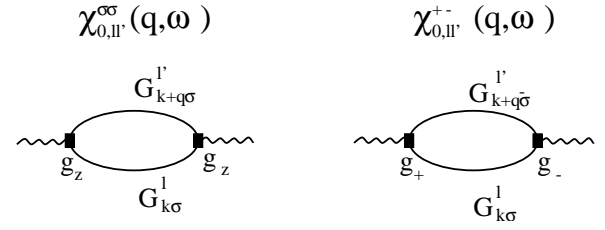


FIG. 2. Diagrammatic representation for the transverse and longitudinal components of the magnetic susceptibility. The full lines represent the electron Green's function with pseudospin and pseudo-orbital-indexes. g_+ and g_z denote the vertices as described in the text.

$$\begin{aligned} c_{k,yz}^+ &= u_{1k} a_{k,yz}^+ + iv_{1k} a_{k,xz}^+ ; \\ c_{k,xz}^+ &= u_{2k} a_{k,yz}^+ + iv_{2k} a_{k,xz}^+ ; \\ c_{k,yz}^+ &= u_{1k} a_{k,yz}^+ + iv_{1k} a_{k,xz}^+ ; \\ c_{k,xz}^+ &= u_{2k} a_{k,yz}^+ + iv_{2k} a_{k,xz}^+ ; \end{aligned} \quad (4)$$

where $u_{mk} = \frac{P}{(t_{k,yz} - t_{k,xz} - A_k)^2 + 2}$ and $v_{mk} = \frac{P}{(t_{k,yz} - t_{k,xz} - A_k)^2 + 2}$. The '-' and '+' signs refer to the $m = 1$ and $m = 2$, respectively.

In Fig. 1 we show the resultant Fermi surfaces for each obtained band where we have chosen $\epsilon_F = 100\text{meV}$ in agreement with earlier estimations [14,17]. One immediately sees that xz - and yz -bands split around the nested parts in good agreement with experiment [18]. Thus, spin-orbit coupling acts as a hybridization between these bands. However, in contrast to hybridization spin-orbit coupling introduces also an anisotropy for the states with pseudo-spins and $\#$. This will be reflected in the magnetic susceptibility. Since the spin and orbital degrees of freedom are now mixed in some spin-orbital liquid, the magnetic susceptibility involves also the orbital magnetism which is very anisotropic.

For the calculation of the transverse, $\chi_{||}^+$, and longitudinal, $\chi_{||}^{zz}$, components of the spin susceptibility of each band we use the diagrammatic representation shown in Fig. 2. Since the Kramers degeneracy is not removed by the spin-orbit coupling, the main anisotropy arises from the calculations of the anisotropic vertex $g_z = \mathbb{I}_z + 2s_z$ and $g_+ = \mathbb{I}_+ + 2s_+$ calculated on the basis of the new quasiparticle states. In addition, due to the hybridization between xz - and yz -bands we also calculate the transverse and longitudinal components of the the interband susceptibility $\chi_{||}^0$. Then, for example,

$$\chi_{0,xz}^+(q;!) = \frac{4}{N} \sum_k (u_{2k} u_{2k+q} - v_{2k} v_{2k+q})^2 \frac{f(\epsilon_{k,xz}^+) - f(\epsilon_{k+q,xz}^+)}{\epsilon_{k,xz}^+ - \epsilon_{k+q,xz}^+ + ! + i0^+} ; \quad (5)$$

and

$$\chi_{0,xz}^{zz}(q;!) = \chi_{xz}^-(q;!) + \chi_{xz}^\#(q;!) = \frac{2}{N} \sum_k$$

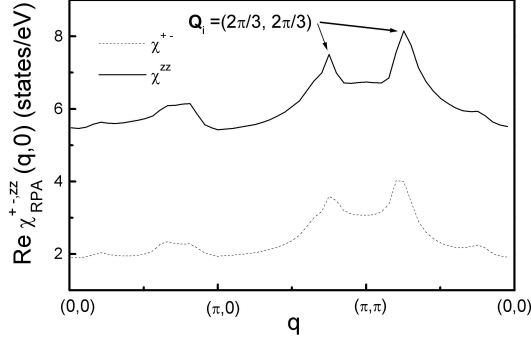


FIG. 3. Results for the real part of the out-of-plane (solid curve) and in-plane (dashed curve) magnetic susceptibilities, $\text{Re } \chi_{\text{RPA}}^{\pm}(q; !)$, calculated within RPA using $U = 0.575\text{eV}$ along the route $(0;0) \rightarrow (\pi;0) \rightarrow (\pi;\pi) \rightarrow (0;0)$ within the first Brillouin Zone at temperature $T = 100\text{K}$.

$$h_{2k} u_{2k+q} + v_{2k} v_{2k+q} + \frac{p_-}{2} (u_{2k} v_{2k+q} + v_{2k} u_{2k+q}) i_2$$

$$\frac{f(k_{xz})}{f(k_{xz} + ! + i0^+)} \frac{f(k_{q+xz})}{f(k_{q+xz} + ! + i0^+)} ; \quad (6)$$

where $f(x)$ is the Fermi function and u_k^2 and v_k^2 are the corresponding coherence factors which we have calculating through the corresponding vertexes using Eq. (4). For all other orbitals the calculations are straightforward. Note, that the magnetic response of the xy -band remains isotropic. One clearly sees the difference between longitudinal and transverse components which results from the calculated matrix elements. Moreover, the longitudinal gets an extra term due to I_z while the transverse does not contain the contributions from I_x or I_y . The latter occur due to the fact that xz - and yz -states are a combination of the real orbital states $|j; +1\rangle$ and $|j; -1\rangle$. Thus the transition between these two states are not possible with I_x or I_y operators. Therefore, each component of the longitudinal susceptibility gets an extra term in the matrix element that sufficiently enhances their absolute values.

Assuming $U_{ij} = \delta_{ij}U$ one gets the following expressions for the transverse susceptibility within RPA:

$$\chi_{\text{RPA}, \perp}^{\pm}(q; !) = \frac{\chi_{0, \perp}^{\pm}(q; !)}{1 - U \chi_{0, \perp}^{\pm}(q; !)} ; \quad (7)$$

and for the longitudinal susceptibility

$$\chi_{\text{RPA}, \parallel}^{\text{ZZ}}(q; !) = \frac{\chi_{0, \parallel}^{\text{ZZ}}(q; !) + \chi_{0, \parallel}^{\#}(q; !) + 2U \chi_{0, \parallel}^{\text{ZZ}}(q; !) \chi_{0, \parallel}^{\#}(q; !)}{1 - U^2 \chi_{0, \parallel}^{\#}(q; !) \chi_{0, \parallel}^{\text{ZZ}}(q; !)} ; \quad (8)$$

In Fig. 3 we show the results for the real part of the transverse and longitudinal total susceptibility, $\chi_{\text{RPA}}^{\pm, \text{ZZ}} =$

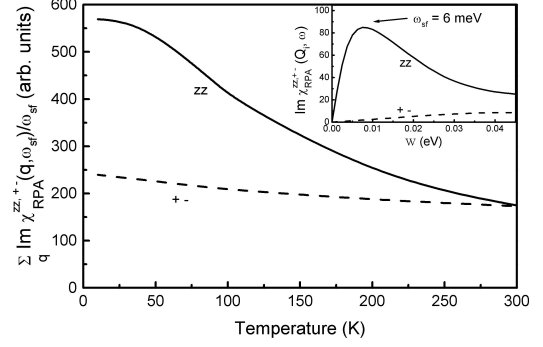


FIG. 4. Temperature dependence of the imaginary part of the spin susceptibility divided by $!_{\text{sf}}$ and summed over q . Note, zz and $+$ refer to the out-of-plane (solid curve) and in-plane (dashed curve) components of the RPA spin susceptibility. In the inset we show the corresponding frequency dependence of the $\text{Im } \chi_{\text{RPA}}^{\pm}(Q_i; !)$ at the IAF wave vector $Q_i = (2\pi/3; 2\pi/3)$. The results for the out-plane component (solid curve) are in a quantitative agreement with INS experiments [6].

$\chi_{\text{RPA}, \parallel}^{\text{ZZ}}$ along the route $(0;0) \rightarrow (\pi;0) \rightarrow (\pi;\pi) \rightarrow (0;0)$ in the first Brillouin Zone for $U = 0.505\text{eV}$. Note, the important difference between the two components. The longitudinal component of the spin susceptibility is almost three times larger than the transverse one all over the Brillouin Zone. Moreover, despite of some structure seen in χ_{RPA}^{\pm} at $(2\pi/3; 2\pi/3)$ there are no real incommensurate antiferromagnetic fluctuations at this wave vector. On the other hand, the structure in $\chi_{\text{RPA}}^{\text{ZZ}}$ at the same wave vector refers to real fluctuations. The latter is seen in the inset of Fig. 4 where we present the results for the frequency dependence of the imaginary part of the total susceptibilities at $Q_i = (2\pi/3; 2\pi/3)$ and temperature $T = 20\text{K}$. The longitudinal component reveals a peak at approximately $!_{\text{sf}} = 6\text{meV}$ in quantitative agreement with experimental data on INS [6]. The transverse component is featureless showing the absence of the incommensurate antiferromagnetic spin fluctuations. Thus, the fluctuations in the transverse susceptibility are isotropic and ferromagnetic-like. Therefore, antiferromagnetic fluctuations are present only perpendicular to the RuO_2 plane.

We also note that our results are in accordance with earlier estimations made by Ng and Sigrist [19] with one important difference. In their work it was found that the IAF are slightly enhanced in the longitudinal components of the xz - and yz -bands in comparison to the transverse one. In our case we have found that the longitudinal component of the magnetic susceptibility strongly enhances due to orbital contributions. Moreover, we show by taking into account the correlation effects within random-phase approximation (RPA) the IAF are further enhanced in the z -direction.

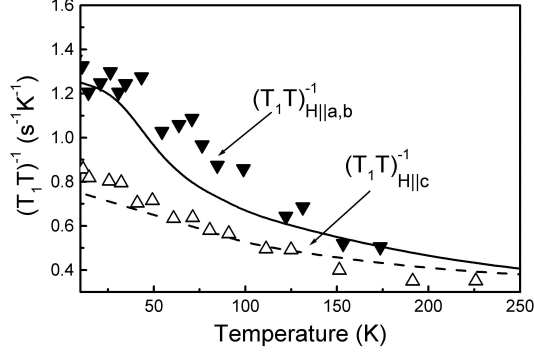


FIG. 5. Calculated normal state temperature dependence of the nuclear spin-lattice relaxation rate T_1^{-1} of ^{17}O in the RuO_2 -plane for the external magnetic field applied along c-axis (dashed curve) and along the ab-plane (solid curve). Down- and up-triangles are experimental points taken from Ref. [13] for the corresponding magnetic field direction.

In order to see the temperature dependence of the magnetic anisotropy induced by the spin-orbit coupling we display in Fig. 4 the temperature dependence of the quantity $\frac{\text{Im}_{\text{RPA}}(q; i_{\text{sf}})}{i_{\text{sf}}}$ for both components. At room temperatures both longitudinal and transverse susceptibilities are almost identical, since thermal effects wash out the influence of the spin-orbit interaction. With decreasing temperature the magnetic anisotropy arises and at low temperatures we find the important result that the out-of-plane component $^{\text{zz}}$ is about two times larger than the in-plane one ($^{\text{zz}} > ^{\text{+}} = 2$).

Finally, in order to compare our results with experimental data we calculate the nuclear spin-lattice relaxation rate for ^{17}O ion in the RuO_2 -plane for different external magnetic field orientation ($i = a; b$; and c)

$$\frac{1}{T_1 T} = \frac{2k_B}{(\hbar)^2} \frac{\chi_n}{q} A_q^{\text{p}} \frac{\text{Im}_{\text{RPA}}(q; i_{\text{sf}})}{i_{\text{sf}}}; \quad (9)$$

where A_q^{p} is the q -dependent hyperfine-coupling constant perpendicular to the i -direction.

In Fig. 5 we show the calculated temperature dependence of the spin-lattice relaxation for an external magnetic field within and perpendicular to the RuO_2 -plane together with experimental data. At $T = 250\text{K}$ the spin-lattice relaxation rate is almost isotropic. Due to the anisotropy in the spin susceptibilities arising from spin-orbit coupling the relaxation rates become different with decreasing temperature. The largest anisotropy occurs close to the superconducting transition temperature in good agreement with experimental data [13].

To summarize, our results clearly demonstrate the essential significance of spin-orbit coupling for the spin-dynamics already in the normal state of the triplet superconductor Sr_2RuO_4 . We find that the magnetic response becomes strongly anisotropic even within a RuO_2 -plane:

while the in-plane response is mainly ferromagnetic, the out-of-plane response is antiferromagnetic-like.

Let us also remark on the implication of our results for the triplet superconductivity in Sr_2RuO_4 . In a previous study [11], neglecting spin-orbit coupling but including the hybridization between xy - and xz ; yz -bands, we have found ferromagnetic and IAF fluctuations within the ab-plane. This would lead to nodes within the RuO_2 -plane. However, due to the magnetic anisotropy induced by spin-orbit coupling, a nodeless p wave pairing is possible in the RuO_2 -plane as experimentally observed. Our results provide further evidence for the importance of spin fluctuations for triplet superconductivity in Sr_2RuO_4 .

We are thankful for stimulating discussions with B. L. Gyor'y, Y. M. Aeno, D. Fay, M. Erem'in, R. Tarento and M. O. Vchinnikova for critical reading of the manuscript. We are grateful to German-French Foundation (PRO-COPE) for the financial support. The work of I. E. is supported by the Alexander von Humboldt Foundation and CRDF Grant No. REC.007.

-
- [1] Y. M. Aeno et al., Nature 372, 532 (1994).
 - [2] K. Ishida et al., Phys. Rev. B 56, R505 (1997).
 - [3] J. A. Du y et al., Phys. Rev. Lett. 85, 5412 (2000).
 - [4] M. A. Tanatar, M. Suzuki, S. Nagai, Z. Q. Mao, Y. M. Aeno, and T. Ishiguro, Phys. Rev. Lett. 86, 2649 (2001).
 - [5] K. Izawa, H. Takahashi, H. Yamaguchi, Y. Matsuda, M. Suzuki, T. Sasaki, T. Fukase, Y. Yoshida, R. Settai, and Y. Onuki, Phys. Rev. Lett. 86, 2649 (2001).
 - [6] Y. Sidis et al., Phys. Rev. Lett. 83, 3320 (1999).
 - [7] H. Mukuda et al., J. Phys. Soc. Jpn. 67, 3945 (1998).
 - [8] I. I. Mazin and D. J. Singh, Phys. Rev. Lett. 82, 4324 (1999).
 - [9] M. E. Zhitomirsky, and T. M. Rice, Phys. Rev. Lett. 87, 057001 (2001).
 - [10] J. F. Annett, G. Litak, B. L. Gyor'y, and K. J. W. Yoskinsi, cond-mat/0109023 (unpublished).
 - [11] I. Erem'in, D. Manske, C. Joas, and K. H. Bennemann, cond-mat/0102074 (unpublished).
 - [12] F. Servant, S. Raymond, B. Fak, P. Lejay, and J. Flouquet, Solid State Commun. 116, 489 (2000).
 - [13] K. Ishida, H. Mukuda, Y. Minami, Y. Kitaoka, Z. Q. Mao, H. Fukazawa, and Y. M. Aeno, Phys. Rev. B 64, 100501 (R) (2001).
 - [14] K. K. Ng, and M. Sigrist, Europhys. Lett. 49, 473 (2000).
 - [15] A. Liebsch, and A. Lichtenstein, Phys. Rev. Lett. 84, 1591 (2000).
 - [16] D. K. Morr, P. F. Trautman, and M. J. Graf, Phys. Rev. Lett. 86, 5978 (2001).
 - [17] T. Mizokawa, L. H. Tjeng, G. A. Sawatzky, G. Ghiringhelli, O. Tjernberg, N. B. Brookes, H. Fukazawa, S. Nakatsuji, and Y. M. Aeno, Phys. Rev. Lett. 87, 077202 (2001).

- [18] A. Damascelli et al., Phys. Rev. Lett. 85, 5194 (2000).
- [19] K. K. Ng, and M. Sigrist, J. Phys. Soc. Jpn. 69, 3764 (2000).